

# Wavefront sensing using diffractive elements

Manuel P. Cagigal and Pedro J. Valle\*

Departamento de Física Aplicada, Universidad de Cantabria, Los Castros S/N 39005 Santander, Spain

\*Corresponding author: vallep@unican.es

Received June 29, 2012; revised July 20, 2012; accepted July 23, 2012;  
posted July 23, 2012 (Doc. ID 171676); published September 7, 2012

In this Letter, we introduce a wavefront slope sensor based on a diffractive element. The diffractive element wavefront sensor (DEWS) produces four double overlapping copies of the incoming wavefront acting like a combination of shearing and pyramidal sensors. The DEWS allows a simple and fast slope estimate. The wavefront sampling can be as high as the number of pixel assigned to cover a wavefront copy, and it can be modified with only binning the CCD pixels. The theory for designing the sensor, its application to extract local slope information, and a simple noise analysis are presented. An application example for atmosphere aberrated wavefronts is demonstrated. © 2012 Optical Society of America

OCIS codes: 010.7350, 050.1970, 010.1330.

Wavefront sensing is of great interest in many fields such as astronomy, microscopy, laser communications, optical testing, and human vision. Among the different wavefront sensing techniques, some are based on diffractive optical elements like the lateral shearing interferometer [1] or the holographic wavefront sensor [2]. In a previous paper [3], we introduced a simple and intuitive method for designing diffractive optical elements based on the use of wavefronts aberrated by simple Zernike polynomials. One of the possible applications of this procedure is to obtain several replicas of the incoming wavefront, allowing an easy control of the replica's number and separation.

In this Letter, we introduce a diffractive element wavefront sensor (DEWS) that is able to provide a direct estimate of the wavefront local derivatives. The new diffractive element provides four double overlapping copies of the incoming pupil field so that local wavefront slopes can be extracted from a proper combination of these images. Although DEWS could be considered similar to the pyramid wavefront sensor [4] or to the optical differentiation wavefront sensor [5], it is based on the superposition of sheared pupil copies like lateral shearing interferometers [1].

The main advantage of the new sensor is that it allows for high-resolution and high-dynamic range slope estimates. In addition, it is much easier to use than other high-resolution wavefront sensors. These features make the DEWS particularly suitable for astronomical applications.

To describe the theoretical principles of the DEWS, let us consider the incoming electric field  $E(x, y) = A \exp[i\phi(x, y)]$ , where  $A$  is the constant amplitude and  $\phi(x, y)$  is the wavefront phase ( $x$  and  $y$  are the usual Cartesian coordinates). We will work within the framework of the scalar diffraction theory. The sensor arrangement consists of a pair of achromatic lenses forming a telescopic system and a diffractive element (DE) mask placed at the intermediate focal plane (Fig. 1). The first lens performs the Fourier transform of the input field, the transformed field is then multiplied by the DE, and then the product is Fourier transformed again onto a detection system (CCD).

A DE providing a copy of the incoming wavefront displaced along the  $x$  axis a distance proportional to parameter  $\alpha$  and a second copy to  $-\alpha$  can be obtained using the mask transmission function (see [3]):

$$M_{1x} = \exp(i\alpha r \cos \theta) + \exp(-i\alpha r \cos \theta) \\ = 2 \cos(\alpha r \cos \theta), \quad (1)$$

where  $r$  and  $\theta$  are the usual polar coordinates over the common focal plane.

Two additional copies can be obtained from the following diffractive element:

$$M_{2x} = i \exp(i\alpha' r \cos \theta) - i \exp(-i\alpha' r \cos \theta) \\ = -2 \sin(\alpha' r \cos \theta). \quad (2)$$

In this case, the displacement is proportional to  $\alpha'$ . In general, we will take  $\alpha'$  slightly larger than  $\alpha$ . Note that one of the copies has a minus sign resulting from the sine dependence. The mask obtained as the addition of the two previous ones becomes:

$$M_x = (M_{1x} + M_{2x})/2 = \cos(\alpha r \cos \theta) - \sin(\alpha' r \cos \theta). \quad (3)$$

This diffractive mask will provide two double overlapping copies of the incoming wavefront along the  $x$  direction. An equivalent development can be carried out for the diffractive element providing copies along the  $y$  direction,

$$M_y = \cos(\alpha r \sin \theta) - \sin(\alpha' r \sin \theta). \quad (4)$$

Except for a normalization constant, the final DE can be obtained as:

$$M = (M_x + M_y)/2. \quad (5)$$

An image of the transmittance typical of this kind of filters is shown in Fig. 2.

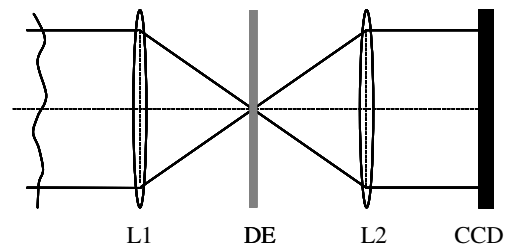


Fig. 1. Set up consisting of a diffractive element (DE) placed at the common focal plane of lenses L1 and L2.

The final field at the CCD plane will be given by:

$$\begin{aligned}
 E_F(x, y) = & E(x, y) * \{ [\delta(x - \alpha) + i\delta(x - \alpha')] \\
 & + [\delta(x + \alpha) - i\delta(x + \alpha')] \\
 & + [\delta(y - \alpha) + i\delta(y - \alpha')] [\delta(y + \alpha) \\
 & - i\delta(y + \alpha')] \}, \quad (6)
 \end{aligned}$$

where  $*$  denotes convolution product and the scale factor  $\lambda f / (2\pi)$  in  $\alpha$  and  $\alpha'$  has been omitted ( $\lambda$  is the wavelength and  $f$  is the lens focal length). In Eq. (6), the convolution product  $E(x, y) * [\delta(x - \alpha) + i\delta(x - \alpha')]$  describes the superposition of two pupil replicas with a relative displacement proportional to  $(\alpha - \alpha')$ , while  $E(x, y) * [\delta(x + \alpha) - i\delta(x + \alpha')]$  the superposition of two replicas with a relative displacement proportional to  $(\alpha' - \alpha)$ . Hence, in the second case, the relative displacement is in the opposite direction to the first one.

To reproduce the transmittance of the DE from Eq. (5), it is necessary to simultaneously use amplitude and phase masks, since this function takes positive and negative values. To simplify manufacturing, it is possible to add a constant offset (and normalization constant) obtaining a final field of the form:

$$\begin{aligned}
 E_F(x, y) = & E(x, y) * \{ [\delta(x - \alpha) + i\delta(x - \alpha')] + [\delta(x + \alpha) \\
 & - i\delta(x + \alpha')] + [\delta(y - \alpha) + i\delta(y - \alpha')] \\
 & \times [\delta(y + \alpha) - i\delta(y + \alpha')] + \delta(0) \}. \quad (7)
 \end{aligned}$$

The term with  $\delta(0)$  provides a central copy of the entrance pupil, as can be seen in Fig. 3, which can be used to estimate the amplitude of the incoming field.

The intensity resulting from the superposition of the two copies of the entrance pupil placed on the positive  $x$  axis (see Fig. 3) is given by:

$$\begin{aligned}
 I_{x+} = & A^2 | \exp[i\phi(x - \alpha, y)] + i \exp[i\phi(x - \alpha', y)] |^2 \\
 = & A^2 \{ 2 + 2 \sin[\phi(x - \alpha, y) - \phi(x - \alpha', y)] \}. \quad (8)
 \end{aligned}$$

The intensity resulting from the superposition with opposite signs of the two copies placed on the negative  $x$  axis is given by:

$$\begin{aligned}
 I_{x-} = & A^2 | \exp[i\phi(x + \alpha, y)] - i \exp[i\phi(x + \alpha', y)] |^2 \\
 = & A^2 \{ 2 + 2 \sin[\phi(x + \alpha', y) - \phi(x + \alpha, y)] \}. \quad (9)
 \end{aligned}$$

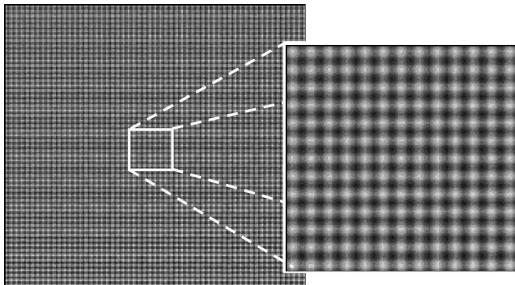


Fig. 2. Typical diffractive mask transmittance function.

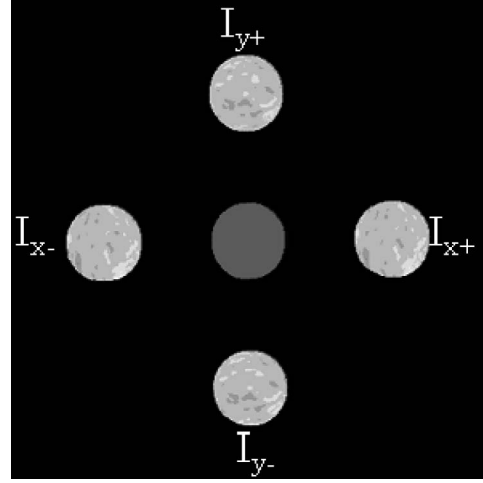


Fig. 3. Simulated image where four pupil copies used for estimating the  $x$  and  $y$  wavefront derivatives simultaneously appear.

Now, taking into account that  $\Delta_x \phi = \Delta_{x+} \phi - \Delta_{x-} \phi$ , where

$$\begin{aligned}
 \Delta_{x+} \phi = & \phi(x - \alpha, y) - \phi(x - \alpha', y) \\
 \Delta_{x-} \phi = & \phi(x + \alpha, y) - \phi(x + \alpha', y), \quad (10)
 \end{aligned}$$

we can combine both intensities to obtain

$$\sin(\Delta_x \phi) = \frac{I_{x+} + I_{x-}}{2A^2} - 2 \approx \Delta_x \phi. \quad (11)$$

Equation (11) provides the phase difference between two points of the pupil plane. The distance between these points is  $\Delta x = 2(\alpha' - \alpha)$  and can be as small as needed. Hence, the wavefront  $x$  derivative can be approximated by:

$$\phi'_x = \Delta_x \phi / \Delta x = \left( \frac{I_{x+} + I_{x-}}{4A^2} - 1 \right) / (\alpha' - \alpha). \quad (12)$$

An equivalent expression for the wavefront  $y$  derivative is attained from the intensities distributed along the  $y$  axis. This approach can be considered a high-resolution estimate of the local wavefront derivative, so that the wavefront is only limited by the number of pixels of the CCD assigned to the pupil area.

In a previous paper [3], we experimentally showed how these kinds of diffractive masks are able to duplicate images. Hence, now we only check the technique by means of computer simulations. As an example, we have applied the DEWS to estimate the slopes of an atmospherically aberrated wavefront. Computer simulations were carried out using the FFT routine implemented in Matlab. To achieve a good spatial sampling and to avoid aliasing effects,  $1024 \times 1024$  data samples were used. The telescope pupil was simulated with a  $128 \times 128$  data sampling. We simulated series of  $\phi(x, y)$  for a number of atmospheric conditions following the standard procedure established by Rodier [6], using 560 Zernike polynomials. In all cases, piston, tip, and tilt were corrected. If we introduce any offset in the diffractive mask function, the final image obtained at the CCD plane contains five copies as Fig. 3 shows. Since a part of the incoming energy is addressed

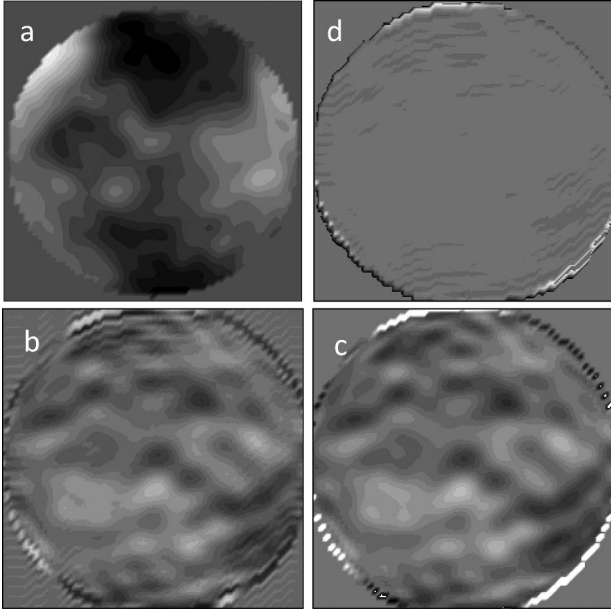


Fig. 4. (a) Incoming wavefront with  $D/r_0 = 5$ . (b) Wavefront  $x$  derivative estimated applying Eq. (12). (c) Actual wavefront  $x$  derivative. (d) Difference between actual and estimated.

to the central copy, the light intensity of the noncentral copies decreases and background and detection noise may affect the derivative estimate to a larger extent.

The wavefront  $x$  derivative is estimated introducing the simulated intensities  $I_{x+}$  and  $I_{x-}$  into Eq. (12). A particular case of wavefront  $x$  derivative estimate for a simulated wavefront with  $D/r_0 = 5$ , where  $D$  is the pupil diameter and  $r_0$  is the Fried parameter, is shown in Fig. 4. It can be seen that both estimated [Fig. 4(b)] and actual [Fig. 4(c)]  $x$  derivatives are quite similar in spite of the fact that some interferences affect the borders of the estimated one. This is more evident in Fig. 4(d), which shows the difference between the two wavefront  $x$  derivatives. The relative error of the estimate derivative is about 5%. Although we only show a result concerning the  $x$  derivative, it is obvious that identical results can be obtained for the  $y$  wavefront derivative.

An interesting feature of the DEWS is its high resolution, since it only depends on the number of pixels assigned to the area covered for the pupil replica. Besides, with a simple binning operation, the resolution may be reduced. This, as we will see later, can be useful to increase the signal-to-noise ratio (SNR) of the slope estimate.

Since manufacturing continuous pupil functions may be difficult and expensive, we also tested binary DE obtained assigning transmittance 1 to all points of the continuous mask with a value above a threshold and transmittance zero to the others. The estimated slopes are the same as those obtained from continuous masks, but a little noisier. We also checked that phase-only DE obtained by introducing the result of Eq. (5) in a complex exponential ( $PM = \exp(iM)$ ) provides the same results as amplitude-only masks [3].

To optimize the parameters involved in the design of the wavefront sensor, we evaluated the SNR of the slope estimate when using Eq. (12). The total intensity at a particular detection area of the sensor can be expressed as the sum of the intensities of the  $N_P$  pixels contained in

that detection area. Its variance, using the standard error propagation formula, can be written as:

$$\sigma_{rn}^2 = N_P [2A^2(\alpha' - \alpha)]^{-2} \sigma_r^2, \quad (13)$$

where  $\sigma_r$  is the read noise error of the CCD. Consequently, the SNR for the sensor when only read noise is considered can be expressed as:

$$\text{SNR}_{rn} = \frac{\langle \phi' \rangle}{\sqrt{N_P}} \frac{2A^2(\alpha' - \alpha)}{\sigma_r}, \quad (14)$$

where  $\langle \dots \rangle$  means ensemble average.

To evaluate the SNR when only photon noise is considered, we apply the standard error propagation expression to Eq. (12):

$$\sigma_{pn}^2 = [2A^2(\alpha' - \alpha)]^{-2} \sigma_I^2, \quad (15)$$

where  $\sigma_I^2$  is the intensity variance. Then, the SNR, when the detection is affected only by Poisson noise, will be:

$$\text{SNR}_{pn} = \langle \phi' \rangle 2(\alpha' - \alpha) \sqrt{n_P}, \quad (16)$$

where  $A^2 = n_P$  is the number of photons arriving at the corresponding sensor area and  $\sigma_I^2 = n_P$ .

Equations (14) and (16) show that both SNR increase when the distance between the two overlapping pupils increases, although the derivative estimate would be less accurate. Hence, a constraint for designing the sensor is that a balance between SNR and accuracy has to be found. This balance can be attained by modifying the distance between the overlapping replicas (e.g., by using a set of DEWS of different parameters or a spatial light modulator to generate the masks).

The main drawback is that SNR is limited by the diffractive efficiency of DE that reduces  $n_P$  values. Another limitation comes from the narrow spectral bandwidth of the diffraction elements. Nevertheless, DEWS is particularly interesting for astronomical applications where low diffractive efficiency and narrow spectral bandwidth can be overcome using laser guide stars or intense natural stars.

We have developed the DEWS, a wavefront sensor that allowed simple implementation, detection, and processing. It is based on a diffractive element designed following a procedure experimentally checked in a previous paper. Its main advantage is its high resolution, which can be simply adapted. Results are promising and suggest that DEWS can successfully compete with other high-resolution wavefront sensors.

The authors wish to thank Nicholas Devaney for his constructive comments and suggestions. This research was supported by the Ministerio de Ciencia e Innovación, under project AYA2010-19506.

## References

1. J. Primot and L. Sogno, *J. Opt. Soc. Am. A* **12**, 2679 (1995).
2. M. A. A. Neil, M. J. Booth, and T. Wilson, *J. Opt. Soc. Am. A* **17**, 1098 (2000).
3. P. J. Valle and M. P. Cagigal, *Opt. Lett.* **37**, 1121 (2012).
4. R. Ragazzoni, *J. Mod. Opt.* **43**, 289 (1996).
5. J. E. Oti, V. F. Canales, and M. P. Cagigal, *MNRAS* **360**, 1448 (2005).
6. N. Rodier, *Opt. Eng.* **29**, 1174 (1990).